Check for updates

Protection Mechanism against Photocorrosion of GaN Photoanodes Provided by NiO Thin Layers

Jumpei Kamimura, Melanie Budde, Peter Bogdanoff,* Carsten Tschammer, Fatwa F. Abdi, Roel van de Krol, Oliver Bierwagen, Henning Riechert, and Lutz Geelhaar*

The photoelectrochemical properties of n-type Ga-polar GaN photoelectrodes covered with NiO layers of different thicknesses in the range 0–20 nm are investigated for aqueous solution. To obtain layers of well-defined thickness and high crystal quality, NiO is grown by plasma-assisted molecular-beam epitaxy. Stability tests reveal that the NiO layers suppress photocorrosion. With increasing NiO thickness, the onset of the photocurrent is shifted to more positive voltages and the photocurrent is reduced, especially for low bias potentials, indicating that hole transfer to the electrolyte interface is hindered by thicker NiO layers. Furthermore, cathodic transient spikes are observed under intermittent illumination, which hints at surface recombination processes. These results are inconsistent with the common explanation of the protection mechanism that the band alignment of GaN/NiO enables efficient hole-injection, thus preventing hole accumulation at the GaN surface that would lead to anodic photocorrosion. Interestingly, the morphology of the etch pits as well as further experiments involving the photodeposition of Ag indicate that photocorrosion of GaN photoanodes is related to reductive processes at threading dislocations. Therefore, it is concluded that the NiO layers block the transfer of photogenerated electrons from GaN to the electrolyte interface, which prevents the cathodic photocorrosion.

Photoelectrochemical (PEC) water splitting is a clean method to produce hydrogen from water using sunlight.[1–3] Since the initial demonstration of this effect using TiO_2 photoelectrodes,[4] worldwide research efforts have been devoted to finding materials that are both stable and enable a high conversion efficiency. Among others, GaN and related alloys, which have been developed for blue light-emitting diodes and lasers,[5–7] are promising candidates for photoelectrodes. This prospect is related to the direct bandgap of these alloys, which provides a large absorption coefficient of $\approx 10^5\ cm^{-1}$ and can be tuned from absorbing in the ultraviolet to the near-infrared region by increasing the In content.[8,9] In addition, the conduction and valence band edges of (In,Ga)N have been calculated to straddle the H^+/H_2 and O_2/H_2O redox potentials for In contents of up to about 50%.[10] However, in the case of n-type $In_xGa_{1-x}N$ photoanodes, photocorrosion has been observed.[11–15] At the same time, p-type $In_xGa_{1-x}N$ alloys are known as stable photocathodes, but there are difficulties in growth because these alloys are due to unintentional doping normally n-type.[15,16]

Several protective layers and catalysts have been tested for such photoanodes to suppress photocorrosion.[17–25] In particular, the loading of p-type NiO cocatalysts enhances the stability of GaN during the oxygen evolution reaction (OER).[19–25] However, the mechanism of the protection against photocorrosion is not well understood. Thus, the goal of this study is to investigate the protection mechanism. To this end, we prepare a series of epitaxial NiO thin films with different thicknesses on GaN templates by plasma-assisted molecular beam epitaxy (PA-MBE). This technique allows a more precise control of the film thickness and a higher crystalline quality than spin coating, which is conventionally used for NiO loading onto GaN. We systematically study the protection mechanism by means of cyclic voltammetry, potentiostatic photocurrent measurements, and photodeposition of Ag to identify reduction sites.[26,27]

The starting point for our investigation of the protection mechanism is cyclic voltammetry measurements of the GaN photoelectrodes with NiO layers of various thicknesses, carried out with 1 M NaOH as the electrolyte. **Figure 1**a shows the

Dr. J. Kamimura, M. Budde, C. Tschammer, Dr. O. Bierwagen, Prof. H. Riechert, Dr. L. Geelhaar
Paul-Drude-Institut für Festkörperelektronik
Leibniz-Institut im Forschungsverbund Berlin e.V.
Hausvogteiplatz 5–7, 10117 Berlin, Germany
E-mail: jumpei.kamimura@gmail.com

Dr. P. Bogdanoff, Dr. F. F. Abdi, Prof. R. van de Krol
Institute for Solar Fuels
Helmholtz-Zentrum Berlin für Materialien und Energie GmbH
Hahn-Meitner-Platz 1, Berlin 14109, Germany
E-mail: bogdanoff@helmholtz-berlin.de

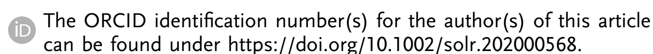
The ORCID identification number(s) for the author(s) of this article can be found under https://doi.org/10.1002/solr.202000568.

© 2020 The Authors. Solar RRL published by Wiley-VCH GmbH. This is an open access article under the terms of the Creative Commons Attribution License, which permits use, distribution and reproduction in any medium, provided the original work is properly cited.

The copyright line for this article was changed on 17 November 2020 after original online publication and Projekt Deal funding statement was added.

DOI: 10.1002/solr.202000568

2367198x, 2020, 12, Downloaded from https://onlinelibrary.wiley.com/doi/10.1002/solr.202000568 by Technische Informationsbibliothek, Wiley Online Library on [05/12/2022]. See the Terms and Conditions (https://onlinelibrary.wiley.com/terms-and-conditions) on Wiley Online Library for rules of use; OA articles are governed by the applicable Creative Commons License

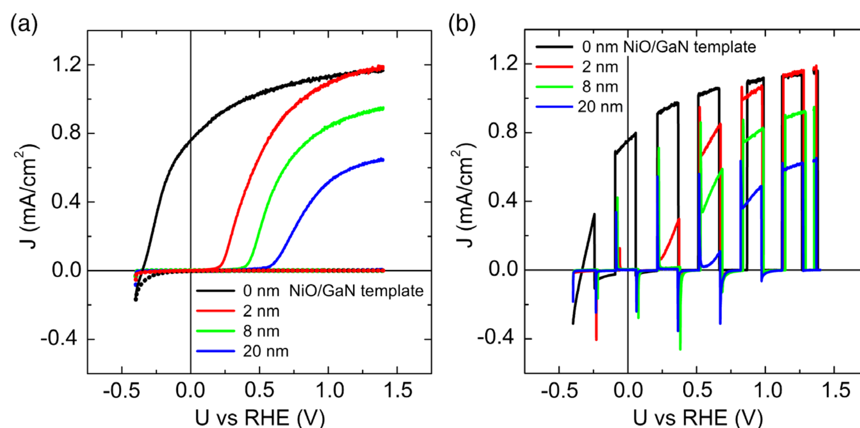

Figure 1. a) Current–voltage curves obtained from cyclic voltammetry measurements for GaN photoelectrodes with NiO layers of different thicknesses (as described in the legend), acquired with 1 M NaOH as the electrolyte in the dark (dotted lines) and under illumination (solid lines, Xe lamp with intensity ≈100 mW cm^{-2}). b) Current–voltage curves for analogous samples, acquired under chopped illumination.

corresponding current–voltage (J–V) curves acquired in the dark and under illumination (Xe lamp with intensity ≈100 mW cm^{-2}). As a reference, data for a GaN photoelectrode without any NiO are also shown. The dark current is negligible for all samples. Under illumination, the onset of the photocurrent shifts toward more positive voltages and the maximum photocurrent decreases with increasing NiO thickness. The shifts of the photocurrent onset can be explained by the competition of interface recombination processes due to interface traps with slow kinetics of the OER.[28] Indeed, we observed transient photocurrent spikes under chopped light conditions for the samples with NiO layer (Figure 1b), which is a direct consequence of interface recombination processes. These recombination processes can occur either at the GaN/NiO or at the NiO/electrolyte interface. As Ni-oxides are known to be efficient catalysts for the OER in alkaline electrolytes, the first option seems to be the more likely reason for these photocurrent transients. With increasing positive potential, the recombination traps filled with electrons are depopulated and the current rises rapidly. The decrease in the maximum achieved photocurrent is probably caused by the high resistivity of the NiO layers[29] because they were grown without intentional doping. The NiO layers hinder hole transfer from GaN to the electrolyte, which leads to an increase in bulk recombination in the GaN or NiO and a concomitant decrease in photocurrent. We note that light absorption in the NiO film could also play a role in the reduction of the photocurrent. However, the almost linear dependence of the maximum photocurrent on the NiO film thickness and estimations of light absorption in NiO indicate that the electrical resistivity is the decisive factor.

To investigate the stability of the samples during the OER, we carried out potentiostatic photocurrent measurements at 1.2 V_{RHE}. The results are shown in **Figure 2**. After 2 h (7200 s), the electrolyte was renewed, and then the stability test was continued for another 30 min. All samples show a gradual decrease in the photocurrent that is interrupted several times by sudden increases. This behavior can be explained by the formation, accumulation, and detachment of gas bubbles via water oxidation on the sample surface. In fact, after replacement of the electrolyte, the photocurrents recover the original values for all samples.

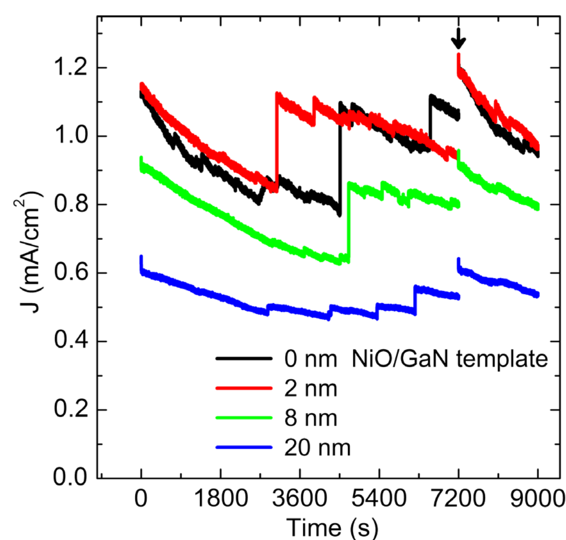

Figure 2. Potentiostatic photocurrent measurements at a bias of 1.2 V_{RHE} for GaN photoelectrodes with NiO layers of different thicknesses as described in the legend, carried out with a Xe lamp with intensity ≈100 mW cm^{-2}. The arrow indicates the time (2 h) at which the electrolyte (1 M NaOH) was renewed.

Hence, judging from only the photocurrent measurements, all samples appear to be stable.

For a more rigorous assessment of the sample stability, we acquired scanning electron microscopy (SEM) images of the sample surfaces after the potentiostatic measurements; these images are shown in **Figure 3**. The GaN surface without any NiO layer seen in Figure 3a is severely etched. The surface of the sample with a 2 nm-thick NiO layer is also corroded, as shown in Figure 3b, but clearly less so, although the total charge density that passed through this sample during the potentiostatic photocurrent measurement (9.2 C cm^{-2}) is larger than for the sample without NiO (8.7 C cm^{-2}). Furthermore, samples with a thicker NiO layer exhibit less surface corrosion, and the surface of the sample with the thickest NiO layer is almost not etched at

© 2020 The Authors. Solar RRL published by Wiley-VCH GmbH

2367198x, 2020, 12, Downloaded from https://onlinelibrary.wiley.com/doi/10.1002/solr.202000568 by Technische Informationsbibliothek, Wiley Online Library on [05/12/2022]. See the Terms and Conditions (https://onlinelibrary.wiley.com/terms-and-conditions) on Wiley Online Library for rules of use; OA articles are governed by the applicable Creative Commons License

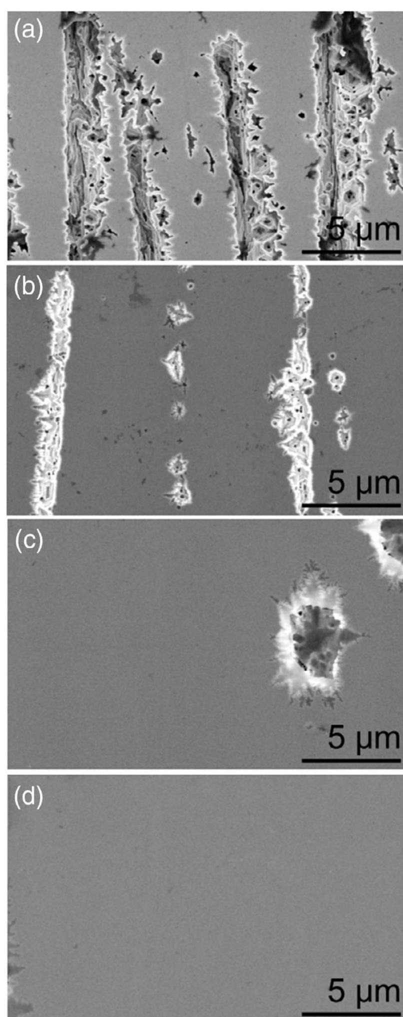

Figure 3. SEM top-view images of the samples after the potentiostatic photocurrent measurements presented in Figure 2. a) Bare GaN photoelectrode without NiO layer. b–d) Samples with a NiO layer of thickness 2, 8, and 20 nm, respectively.

all (Figure 3d). These results indicate that a sufficiently thick NiO layer prevents photocorrosion of GaN. We attribute the apparent stability of the photocurrent in Figure 2 for the samples with a thin or with no NiO layer to a photoetching process which is significantly slower than the simultaneous water oxidation. This assumption is supported by a rough estimation of the maximum possible corrosion impact via the Faraday law. In a corrosion process that consumes three photogenerated charge carriers per GaN unit, a layer of about 4 µm of the photoelectrode would be fully corroded after a charge of $9.2\ \text{C cm}^{-2}$ was flown. This means that most of the 5 µm-thick GaN film would have been etched away. However, such drastic change in the morphology of the photoelectrode could not be observed in our SEM images. This reveals that the majority of the photocurrent can be assigned to the OER and that the photocorrosion is so slow that it can be maintained for a long time in the 5 µm-thick layer.

With respect to the mechanism by which NiO protects GaN from photocorrosion, Kim et al. suggested that the band alignment of these two materials facilitates the transfer of photogenerated holes to the NiO/electrolyte interface, which prevents hole accumulation on the GaN surface and thus anodic photocorrosion.[21–23] However, our results are in conflict with this hypothesis. In particular, we observed photocurrent spikes in our chopped illumination cyclic voltammetry experiments for the samples with NiO layer, but not for the bare GaN (see Figure 1b). Especially the cathodic transient spikes indicate that holes do accumulate at the surface. Nevertheless, the samples with NiO are more stable than the bare GaN. Furthermore, if photogenerated holes were efficiently transferred through the NiO, the photocurrent would not be reduced with increasing NiO thickness.

In a previous study, we proposed that photocorrosion of GaN is not caused by photogenerated holes but photogenerated electrons.[17] We found that loading of GaN with the catalyst cobalt phosphate (Co-Pi) suppresses surface recombination of photogenerated holes and significantly enhances the photocurrent but does not prevent photocorrosion, which excludes that the corrosion is related to photogenerated holes. Instead, corrosion could be reductive, caused by photogenerated electrons that reach the surface via charged threading dislocations despite the surface band bending. In that previous study, we corroborated this suggestion by experiments with H_2O_2, a scavenger for both electrons and holes, in which corrosion was suppressed. Moreover, further evidence was the morphology of the photocorroded surface. As seen also in Figure 3a,b, the etch pits exhibit an elongated form and are arranged along essentially parallel lines. This morphology implies that etching starts at macrostep edges. Such macrosteps can form by step bunching on off-axis sapphire substrates, and it is known that threading dislocations are preferentially located along such macrostep edges.[30–32]

To investigate reductive corrosion further, we analyze now the photodeposition of Ag on GaN photoelectrodes with and without NiO layers. The SEM images in **Figure 4**a,b reveal that on bare GaN, Ag nanoparticles nucleate via the reduction of Ag^+ by photogenerated electrons preferentially along the macrostep edges and form flower-like structures. These nanoparticles indicate the position of reductive sites on the GaN surface, as explained in Experimental Section. Importantly, the arrangement of the Ag nanoparticles correlates well with the morphology of the etch pits (see Figure 3a). In contrast, Figure 4c,d shows that on GaN with an 8 nm-thick NiO film, Ag is not deposited at all on the surface, except for the sample edges.

All of our results can be explained by the following mechanism. The corrosion process at Ga-polar GaN(0001) takes place via photogenerated electrons which reach the electrolyte/GaN interface via threading dislocations. The reaction mechanism could, in principle, be analogous to the Mars vam Krevelen mechanism, which was theoretically simulated for various transition metal nitrides.[33] The transition metal is reduced and lattice nitrogen is released as NH_3. For GaN, the following reaction equation could be assumed

$$\mathrm{GaN} + 3\mathrm{H_2O} + 3e^- \rightarrow \mathrm{Ga} + \mathrm{NH_3} + 3\mathrm{OH}^- \quad (1)$$

NiO deposited on GaN acts as an electron blocking layer which prevents electron transfer to the interface with the electrolyte. Thus, reductive etching related to photogenerated electrons is suppressed. The blocking of electrons is consistent with the facts

© 2020 The Authors. Solar RRL published by Wiley-VCH GmbH

2367198x, 2020, 12, Downloaded from https://onlinelibrary.wiley.com/doi/10.1002/solr.202000568 by Technische Informationsbibliothek, Wiley Online Library on [05/12/2022]. See the Terms and Conditions (https://onlinelibrary.wiley.com/terms-and-conditions) on Wiley Online Library for rules of use; OA articles are governed by the applicable Creative Commons License

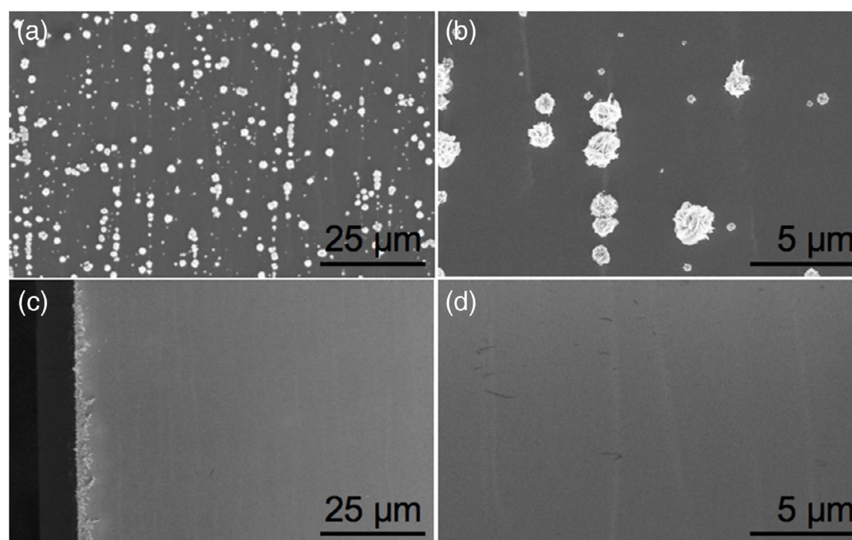

Figure 4. SEM top-view images of GaN photoelectrodes with and without NiO layer after photodeposition of Ag for 3 min. a) Low- and b) high-magnification image for a bare GaN photoelectrode without NiO layer. c) Low- and d) high-magnification image for a sample with an 8 nm-thick NiO layer.

that the band alignment of NiO/GaN is type II with the band edges of p-type NiO lying higher in energy and that the conduction band offset has been reported in the range 1.7–2.7 eV (depending on the position of the Fermi levels).[34,35] Photogenerated holes, on the contrary, can reach the interface with the electrolyte via the valence band of NiO and contribute to the OER. Due to the low conductivity of NiO, this transport and thereby the OER are strongly dependent on the thickness of NiO. In addition, recombination processes at the NiO/GaN interface as well as possibly in the bulk of NiO or GaN also occur in competition with water oxidation.

In principle, the suppression of cathodic photocorrosion could also be explained by the efficient transport of electrons in the NiO layer from the threading dislocations to the electrical contact. We can exclude this scenario because we can infer from another study that the NiO layers are highly resistive and that the remaining low conductivity is p-type.[29] Therefore, the only explanation for all experimental results is that NiO layers block the transfer of electrons from GaN to the electrolyte interface.

Based on the aforementioned explanations, the measured photocurrent is composed of the positive anodic current for water oxidation and the negative cathodic current for photocorrosion. Thereby, one would initially expect that a suppression of the photocorrosion should, in principle, lead to an increase in the measured photocurrent. This is, however, not observed for our samples because of two reasons. First, the corrosion current is only a small proportion of the total current. Second, unfortunately, inhibiting the corrosion with NiO deposition introduces an additional series resistance for hole transport to the electrolyte interface. At the same time, this limitation could be overcome by intentional p-type doping of the NiO, for which significant progress has been achieved recently.[36]

In conclusion, epitaxial NiO thin films protect Ga-polar GaN photoanodes from photocorrosion. The protection mechanism can be understood as follows. The photocorrosion of GaN photoelectrodes is a reductive process and facilitated by electrons transferred to the surface via threading dislocations. The NiO layers act as electron blocking layers, thus preventing cathodic photocorrosion. This insight may pave the way to developing more complex protective layers and/or cocatalysts that effectively protect GaN photoanodes from photocorrosion and enable at the same time high photocurrents, leading ultimately to stable photoanodes for efficient solar water splitting. Intentionally p-type doped NiO is a promising candidate.

Experimental Section

A series of nominally undoped NiO protective layers with different thicknesses were grown on GaN templates by PA-MBE. The GaN templates (purchased from Kyma Technologies Inc.) consist of ≈5 µm nominally undoped n-type Ga-polar GaN(0001) layers grown by hydride vapor phase epitaxy on sapphire substrates using AlN buffer layers. The net ionized donor density of the GaN templates is 5×10^{17} cm^{-3}. The NiO thin films were grown at a temperature of 500 °C, as measured by a thermocouple. Ni was sublimed from a high-temperature effusion cell at a temperature of 1380 °C leading to a beam equivalent pressure of 8.5×10^{-9} mbar. Simultaneously, a flux of activated oxygen was supplied by a plasma source operated at a flow rate of 0.5 sccm and an RF plasma power of 300 W. To vary the NiO thickness, growth times of 5000, 2040, and 480 s were chosen. The thickest NiO sample was analyzed by X-ray reflectometry and the thickness was determined to be 20 nm. The thicknesses of the other samples were deduced to be 2 and 8 nm. These thicknesses were chosen to show the evolution of the protection mechanism from a limited stability enhancement already for extremely thin films up to essentially complete prevention of photocorrosion for films with the maximum thickness of 20 nm. More information on the PA-MBE of NiO on GaN and the physical properties of such films is presented elsewhere.[37] In brief, the NiO layers grow epitaxially with an (111) orientation in two rotational domains. The domain size is on the order of 10–20 nm, and the surface roughness about 1 nm. Furthermore, comparable layers grown on insulating MgO(100) substrates were highly resistive, with the remaining conductivity being p-type.[29] X-ray diffraction, X-ray reflectometry, and atomic force microscopy data for samples used in the present study are provided as Supporting Information.

© 2020 The Authors. Solar RRL published by Wiley-VCH GmbH

2367198x, 2020, 12, Downloaded from https://onlinelibrary.wiley.com/doi/10.1002/solr.202000568 by Technische Informationsbibliothek, Wiley Online Library on [05/12/2022]. See the Terms and Conditions (https://onlinelibrary.wiley.com/terms-and-conditions) on Wiley Online Library for rules of use; OA articles are governed by the applicable Creative Commons License

Cyclic voltammetry measurements were performed with a scan rate of 30 mV s^{-1} using a standard three-electrode PEC cell with a platinum wire as the counter electrode, a Ag/AgCl electrode as the reference electrode, 1 M NaOH as the electrolyte, and a Xe lamp (intensity ≈100 mW cm^{-2}) as the light source. A circular area with a diameter of 6 mm on the sample surface was exposed to the electrolyte and illuminated. Potentials versus the Ag/AgCl electrode were converted to the reversible hydrogen electrode (RHE) scale by the equation $U_{RHE} = U_{Ag/AgCl} + 197\ mV + (59\ mV \times pH)$, based on the fact that GaN follows the Nernstian pH response.[38,39] For the surface electrical contact, an In-Ga eutectic was deposited on part of the semiconductor surface, and this contact was not exposed to the electrolyte. For the photodeposition investigation, we used 1 mM $AgNO_3$ solution. The samples were soaked with the solution and irradiated by a Xe lamp with an intensity of ≈100 mW cm^{-2} for 3 min. The photoreduction of Ag can be described as follows

$$Ag^+ + e^- \rightarrow Ag \quad (2)$$

The redox potential of this reaction is +0.8 V versus RHE and therefore more positive than the conduction band of GaN. Thus, the position of the photodeposited Ag particles reveals the reduction sites on the samples.[26,27]

Supporting Information

Supporting Information is available from the Wiley Online Library or from the author.

Acknowledgements

The authors thank M. Feneberg for fruitful discussions, M. Ramsteiner for a critical reading of the manuscript, and H.-P. Schönherr for MBE support. J.K. is grateful for a JSPS Postdoctoral Fellowship for Research Abroad. The growth of NiO was performed in the framework of GraFOx, a Leibniz ScienceCampus partially funded by the Leibniz Association. M.B. gratefully acknowledges financial support by the Leibniz Association. Open access funding enabled and organized by Projekt DEAL.

Conflict of Interest

The authors declare no conflict of interest.

Keywords

GaN, NiO, photoanodes, photoelectrochemistry

Received: September 13, 2020
Revised: October 4, 2020
Published online: November 5, 2020

[1] T. Hisatomi, J. Kubota, K. Domen, *Chem. Soc. Rev.* **2014**, *43*, 7520.
[2] M. G. Walter, E. L. Warren, J. R. McKone, S. W. Boettcher, Q. Mi, E. A. Santori, N. S. Lewis, *Chem. Rev.* **2010**, *110*, 6446.
[3] K. Sivula, R. van de Krol, *Nat. Rev.* **2016**, *1*, 15010.
[4] A. Fujishima, K. Honda, *Nature* **1972**, *238*, 37.
[5] S. Nakamura, *Rev. Mod. Phys.* **2015**, *87*, 1139.
[6] I. Akasaki, *Rev. Mod. Phys.* **2015**, *87*, 1119.
[7] H. Amano, *Prog. Cryst. Growth Charact. Mater.* **2016**, *62*, 126.
[8] J. Wu, W. Walukiewicz, K. M. Yu, J. W. Ager, E. E. Haller, H. Lu, W. Schaff, *Appl. Phys. Lett.* **2002**, *80*, 4741.
[9] Y. Nanishi, Y. Saito, T. Yamaguchi, *Jpn. J. Appl. Phys.* **2003**, *42*, 2549.
[10] P. G. Moses, C. G. Van de Walle, *Appl. Phys. Lett.* **2010**, *96*, 021908.
[11] K. Fujii, T. Karasawa, K. Ohkawa, *Jpn. J. Appl. Phys.* **2005**, *44*, L543.
[12] I. Waki, D. Cohen, R. Lal, U. Mishra, S. P. DenBaars, S. Nakamura, *Appl. Phys. Lett.* **2007**, *91*, 093519.
[13] I. M. Huygens, K. Strubbe, W. P. Gomes, *J. Electrochem. Soc.* **2000**, *147*, 1797.
[14] M. Finken, A. Wille, B. Reuters, M. Heuken, H. Kalisch, A. Vescan, *Phys. Status Solidi B* **2015**, *252*, 895.
[15] J. Kamimura, P. Bogdanoff, J. Lähnemann, C. Hauswald, L. Geelhaar, S. Fiechter, H. Riechert, *J. Am. Chem. Soc.* **2013**, *135*, 10242.
[16] K. Fujii, K. Ohkawa, *Jpn. J. Appl. Phys.* **2005**, *44*, L909.
[17] J. Kamimura, P. Bogdanoff, F. F. Abdi, J. Lähnemann, R. van de Krol, H. Riechert, L. Geelhaar, *J. Phys. Chem. C* **2017**, *121*, 12540.
[18] L. Caccamo, J. Hartmann, X. Wang, H. Zhou, M. S. Mohajerani, S. K. Gurram, G. Bräuer, H.-H. Wehmann, H. Shen, A. Waag, in *E-MRS 2014 Spring Meeting*, Lille, France, May 26–30 **2014**.
[19] T. Hayashi, M. Deura, K. Ohkawa, *Jpn. J. Appl. Phys.* **2012**, *51*, 112601.
[20] K. Ohkawa, W. Ohara, D. Uchida, M. Deura, *Jpn. J. Appl. Phys.* **2013**, *52*, 08JH04.
[21] S. H. Kim, M. Ebaid, J. H. Kang, S. W. Ryu, *Appl. Surf. Sci.* **2014**, *305*, 638.
[22] J. H. Kang, S. H. Kim, M. Ebaid, J. K. Lee, S. W. Ryu, *Acta Mater.* **2014**, *79*, 188.
[23] S. H. Kim, J. H. Kang, S. W. Ryu, *J. Nanosci. Nanotechnol.* **2014**, *14*, 7903.
[24] K. Koike, K. Yamamoto, S. Ohara, T. Kikitsu, K. Ozasa, S. Nakamura, M. Sugiyama, Y. Nakano, K. Fujii, *Int. J. Hydrogen Energy* **2017**, *42*, 9493.
[25] K. Koike, K. Yamamoto, S. Ohara, M. Sugiyama, Y. Nakano, K. Fujii, *J. Electrochem. Soc.* **2016**, *163*, H1091.
[26] R. Li, F. Zhang, D. Wang, J. Yang, M. Li, J. Zhu, X. Zhou, H. Han, C. Li, *Nat. Commun.* **2013**, *4*, 1432.
[27] K. Wenderich, M. Guido, *Chem. Rev.* **2016**, *116*, 14587.
[28] L. M. Peter, *J. Solid State Electrochem.* **2013**, *17*, 315.
[29] M. Budde, C. Tschammer, P. Franz, J. Feld, M. Ramsteiner, R. Goldhahn, M. Feneberg, N. Barsan, A. Oprea, O. Bierwagen, *J. Appl. Phys.* **2018**, *123*, 195301.
[30] X. Q. Shen, H. Matsuhata, H. Okumura, *Appl. Phys. Lett.* **2005**, *86*, 021912.
[31] X. Q. Shen, H. Okumura, H. Matsuhara, *Appl. Phys. Lett.* **2005**, *87*, 101910.
[32] A. V. Kuchuk, P. M. Lytvyn, C. Li, H. V. Stanchu, Y. I. Mazur, M. E. Ware, M. Benamara, R. Ratajczak, V. Dorogan, V. P. Kladko, A. E. Belyaev, G. G. Salamo, *ACS Appl. Mater. Interfaces* **2015**, *7*, 23320.
[33] Y. Abghoui, E. Skulason, *Catal. Today* **2017**, *286*, 78.
[34] K. Fujii, in *Semiconductors and Semimetals*, Vol. *97*, Elsevier **2017**, pp. 139–183.
[35] V. R. Reddy, P. R. S. Reddy, I. N. Reddy, C.-J. Choi, *RSC Adv.* **2016**, *6*, 105761.
[36] J. Y. Zhang, W. W. Li, R. L. Z. Hoye, J. L. MacManus-Driscoll, M. Budde, O. Bierwagen, L. Wang, Y. Du, M. J. Wahila, L. F. J. Piper, T. L. Lee, H. J. Edwards, V. R. Dhanak, K. H. L. Zhang, *J. Mater. Chem. C* **2018**, *6*, 2275.
[37] M. Budde, T. Remmele, C. Tschammer, J. Feldl, P. Franz, J. Lähnemann, Z. Cheng, M. Hanke, M. Ramsteiner, M. Albrecht, O. Bierwagen, *J. Appl. Phys.* **2020**, *127*, 015306.
[38] K. Koike, A. Nakamura, M. Sugiyama, Y. Nakano, K. Fujii, *Phys. Status Solidi C* **2014**, *11*, 821.
[39] S. S. Kocha, M. W. Peterson, D. J. Arent, J. M. Redwing, M. A. Tischler, J. A. Turner, *J. Electrochem. Soc.* **1995**, *142*, L238.

© 2020 The Authors. Solar RRL published by Wiley-VCH GmbH

2367198x, 2020, 12, Downloaded from https://onlinelibrary.wiley.com/doi/10.1002/solr.202000568 by Technische Informationsbibliothek, Wiley Online Library on [05/12/2022]. See the Terms and Conditions (https://onlinelibrary.wiley.com/terms-and-conditions) on Wiley Online Library for rules of use; OA articles are governed by the applicable Creative Commons License